3-Wheel Swerve Drive - *The Trouble with Tribots*

Clem McKown - FRC Team 1640

14-August-2014

Executive Summary

FRC's 2013 change in robot perimeter rules (to 112 inch maximum overall perimeter from the earlier maximum 28 in x 32 in) opened new opportunities for non-rectangular robots. In particular, the new rules reduce the stability penalty for a 3-wheeled robot design vis-à-vis the preceding rules because it allows an expanded wheelbase for a 3-sided chassis.

The primary expected benefit of a 3-wheeled swerve robot over a 4-wheeled is that it enables the use of two CIM motors per swerve module to yield a drive-train with 6 CIM motors overall. 6 drive CIM motors have become the standard for high-performance tank drive robots within FRC.

A 3-wheeled, 6-CIM swerve robot not only complies with FRC's 2013 & 2014 motor limits, but the mass reduction realized by eliminating one swerve module allows for the addition of CIM motors without excessively compromising other robot systems.

Of course, there are expected to be drawbacks to a triangular, 3-swerve chassis as well as benefits. The team intends to build and test a prototype chassis to gain a better understanding of both the benefits and deficits of the concept.

The purpose of this paper is to define the mathematics for controlling a 3-swerve robot, both under chassis-centric and field-centric control.

Chassis Basis

The proposed chassis design has three swerve modules arranged at the apexes of an equilateral triangle. The pivot axes are located 2.700" from the exterior surface of the chassis frame, a distance which allows safe rotation of the pivot (1640's 2013 & 2014 design) without interfering with bumpers, etc. The chassis frame's apexes are truncated to flats also 2.700" from the pivot axis. The designed total perimeter is 111 in, providing the same 1 in safety margin that 1640 used in their 2013 & 2014 chassis. All swerve modules are mounted so that the calibration 0° faces directly away from chassis center-point.

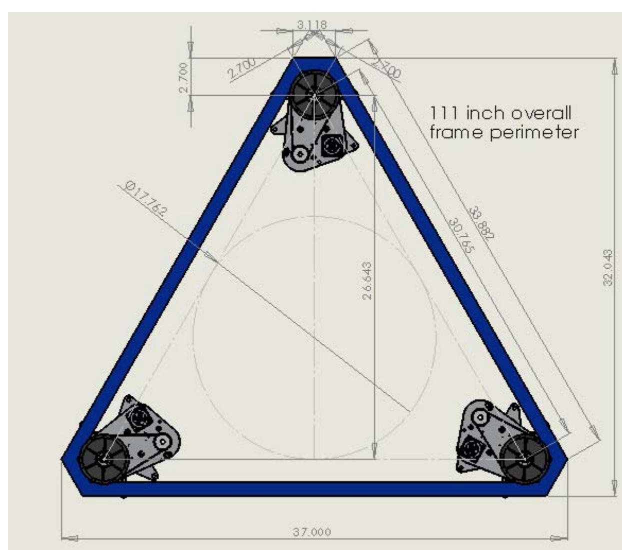

A dimensioned schematic of such a chassis is provided in Figure 1.

Conventions

In this document, lengths will be expressed in inches (in or ") and angles in degrees (°). Longitudinal precision will be 0.001" unless stated otherwise.

Right-hand rule is used in all illustrations for determining positive angle direction. The mathematics will work equally well under left-hand rule, but this must be applied universally. This includes pivot numbering (1, 2, 3). If left-hand rule is used, then 2 & 3 swap positions.

Swerve angles will be based on single-direction drive with each module's drive direction being the swerve angle direction (therefore driving at 0° when the swerve angle is 0°).

Prototype

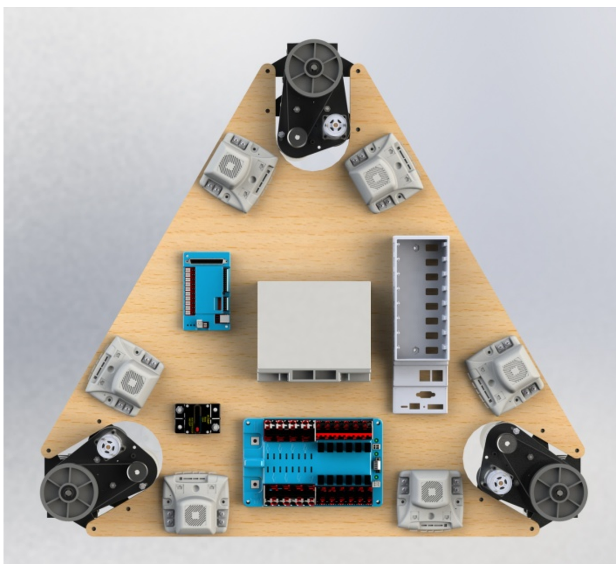

A Tribot prototype chassis was designed and built using 3/4" thick laser-cut plywood. An 8-slot cRIO was employed due to ready availability. Jaguar motor controllers were elected for the same reason. The design called for 2013 swerve modules, but 2012 modules were actually installed, again due to ready availability. The 2012, 2013 & 2014 swerve modules share identical mounting bolt hole patterns (the 2012 having an additional, unused mounting hole) and identical relations between these mounting holes and the pivot, CIM and steering axes, so critical geometry is unaffected. The 2012, 2013 & 2014 swerve modules also utilize the same angle sensors, and these are mounted in the same manner.

The Tribot prototype maintains the same swerve module spacing and orientations as provided in the Figure 1 schematic on Page 1.

Human Interface

The Driver uses a wired Xbox controller having dual, thumb-driven joysticks.

The primary joystick controls the robot's movement in ***Crab Mode***. In ***Crab Mode***, both x and y information is used with the joystick's angle providing directional settings and the joystick's displacement from neutral providing speed settings.

The secondary joystick works with the primary to provide the turning capabilities of ***Snake*** and ***Ocelot Modes***. Only the x information is used from the secondary joystick and this indirectly sets turning radius.

Chassis-centric versus Field-centric control

Chassis-centric and field-centric refer to two different directional references for the driver and the control logic. Team 1640 has hitherto always used chassis-centric control in which a specific axis of the chassis is determined to be "straight ahead". Joystick controls then operate on this reference. This is easier to execute from an instrument and software basis, as it does not require the robot to "know" which way it is facing relative to the field axes. On the other hand, it required the driver to know which way the robot is facing relative to field axis and to put her/his mind into this orientation while driving. This increases the driver's mental burden.

Field-centric control would allow the driver to move the robot around the field using the primary joystick while controlling the chassis orientation relative to the field with the secondary. The driver's reference space becomes the stationary field, reducing (we think) driver's mental burden. From a robot standpoint, life gets harder, as the robot now needs to "know" its orientation relative to the field. Gyroscopes are the way to know this and only one axis is needed. Issue is that the gyroscope must remain stable for the match duration (with all its hard knocks) to be effective.

Other than the change in reference, ***Crab Mode*** remains the same in chassis and field-centric control. The same is not true for ***Snake*** and ***Ocelot***, as these undergo a reversal. In chassis-centric control, ***Snake Mode*** is static whereas ***Ocelot*** requires dynamic driver input. These relationships flip in field-centric control.

Chassis-centric control will be derived first; Field centric follows because it applies an additional level of calculation and control to Chassis-centric logic.

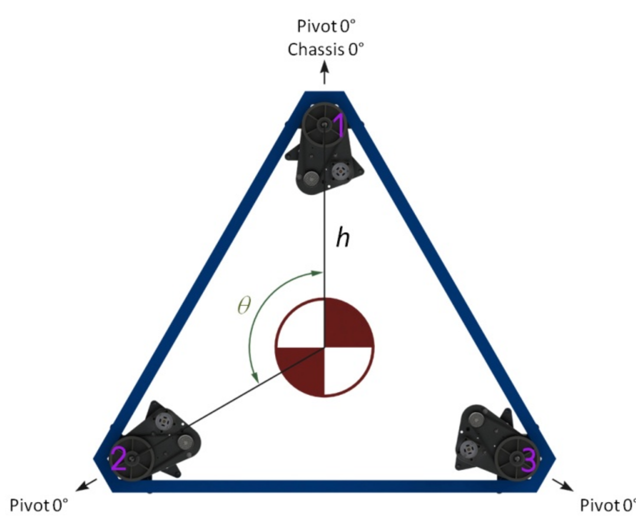

Chassis Geometry

Remaining consistent with both Figure 1 on Page 1, the actual prototype, and (as far as possible) previous white papers by this author, three swerve modules are arranged around a chassis center-point with a uniform distance *h* between the chassis center-point and the pivot axes and an angle $\theta = 120°$ ($2\pi/3R$) between each pivot axis around the chassis center-point. Swerve modules are mounted so that each module's 0° calibration axis faces directly away from the chassis center-point. Swerve modules are identified by numbers 1, 2 & 3 following right-hand rule.

The line from the chassis center-point to the pivot axis of swerve module 1 defines the 0° chassis axis.

Note that based on Figure 1, h = 17.762 in.

Chassis-Centric Crab Mode

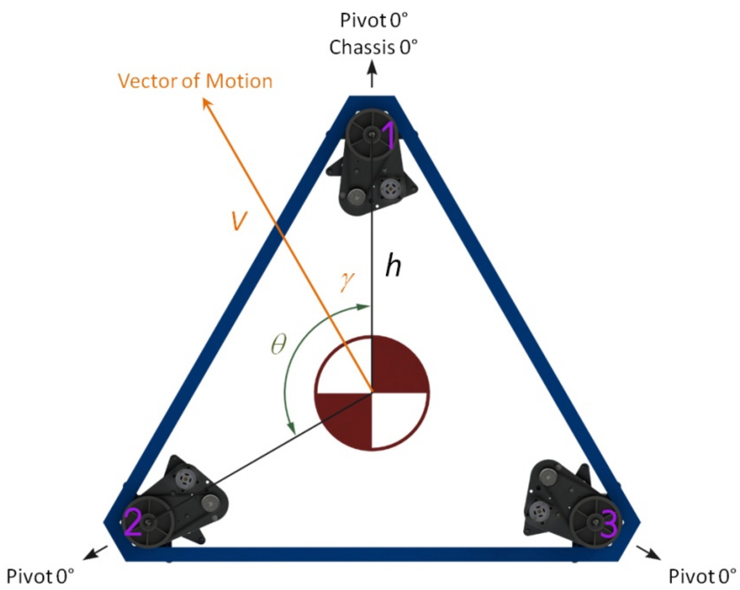

In *Crab Mode*, the primary joystick applies a *Vector of Motion* to the chassis described in the previous section. This *Vector of Motion* provides both angular direction (γ) and power/speed (V) information.

γ may be 0-360°.

For Crab Mode, all swerves would be aligned with γ. For individual swerve angles (α_{Ci}):

$$\alpha_{C1} = \gamma \quad \text{eq. 1}$$

$$\alpha_{C2} = \gamma - 120° \quad \text{eq. 2}$$

$$\alpha_{C3} = \gamma - 240° \quad \text{eq. 3}$$

All calculated swerve angles must be checked and if <0°, add 360° to make >0°. However, the right time to make this correction (and the opposite: if >360°, subtract 360° to make <360°) is after assessing all drive calculations, including ***Snake Mode***.

Drive power (V) is proportional to the primary joystick's displacement from neutral. In ***Crab Mode***, all drives receive equal power.

Chassis-Centric Snake Mode

Snake Mode drives the chassis in an arc with chassis orientation following the path of the arc. The basic chassis orientation and speed are based upon the ***Crab Mode*** primary joystick inputs, while the arc radius is indirectly set via the secondary joystick x input.

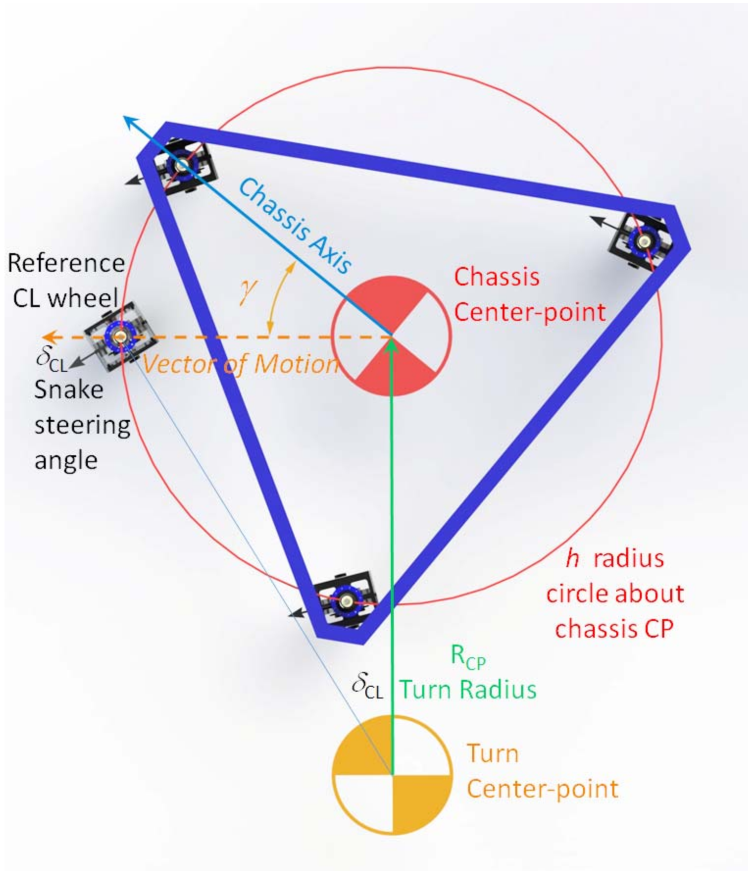

In the 2009 swerve white papers, I introduced the concept of a "reference CL wheel", a useful tool for working through the mathematics around Snake Mode. The "reference CL wheel" concept will be employed again here.

The "reference CL wheel" is not a real wheel, but a hypothetical pivot wheel located at a distance *h* from the chassis center-point and oriented along the *vector of motion*. The diagram at left shows a "reference CL wheel" and the real pivot wheels on a chassis.

The secondary joystick steers by steering the reference CL wheel directly, creating an angle, δ_{CL}, between the *vector of motion* and the reference CL wheel's drive direction. It can be easily shown that the triangle formed by the reference CL wheel, the chassis CP and the Turn CP is a right triangle and has the angle δ_{CL} at the Turn CP apex, which allows calculation of the Turn Radius, R_{CP}.

$$R_{CP} = \frac{h}{\tan \delta_{CL}} \qquad \text{eq. 4}$$

Equation 4 blows up (division by zero) if $\delta_{CL} = 0$ (neutral joystick position). So don't do ***Snake Mode*** calculations if the secondary joystick is neutral.

We need to now define γ_i. γ (no subscript) has already been defined as the angular offset between the chassis axis and the *vector of motion*. γ_i is the angular offset from the *vector of motion* to each individual pivot axis (i = 1, 2, 3). For calculation:

$$\gamma_1 = -\gamma \qquad \text{eq. 5}$$

$$\gamma_2 = 120° - \gamma \qquad \text{eq. 6}$$

$$\gamma_3 = 240° - \gamma \qquad \text{eq. 7}$$

Turn radiuses for all swerve wheels may now be calculated:

$$R_i = \sqrt{h^2 \cos^2 \gamma_i + (R_{CP} - h \sin \gamma_i)^2} \qquad \text{eq. 8}$$

and drive power factors for each wheel:

$$V_i = V \frac{R_i}{R_{\max}} \qquad \text{eq. 9}$$

A choice is now needed. What will be the range of δ_{CL}? In the first *"Pivot-Wheel Drive"* white paper of 2-August-2009, a limited (chassis aligned with *vector of motion*) ***snake mode*** was presented with a δ_{CL} range from -90 to +90°. At the limits of the range, the turn radius is zero and the turn center-point and chassis center-point are the same. Swerve angle calculations were complicated by the need to switch calculations based on whether the turn center-point is inside or outside the wheel-base.

In *"Pivot-Wheel Drive - Crab with a Twist"* white paper of 29-March-2010, a general (random alignment between the chassis and *vector of motion*) ***snake mode*** (referred to as Twist 1 in the paper) was presented, but where δ_{CL}'s range is limited to -45 to 45°. By limiting the range of δ_{CL}, the turn center-point never comes inside of the *h*-radius circle around the chassis center-point; the equations are thereby simplified. The control logic for DEWBOTs IX & X both follow the mathematics presented in this latter paper, including the limited δ_{CL} range.

The math for both cases will be presented here.

For the case that:

[sign of δ_{CL}]·R_{CP} ≥ [sign of δ_{CL}]·$h \sin \gamma_i$ (Turn center-point is not inside wheelbase - always true for $-45° \le \delta_{CL} \le +45°$)

$$\delta_i = [sign\, of\ \delta_{CL}] \sin^{-1} \frac{h \cos \gamma_i}{R_i} \qquad \text{eq. 10}$$

For the case that:

[sign of δ_{CL}]·R_{CP} < [sign of δ_{CL}]·$h \sin \gamma_i$ (Turn center-point is inside wheelbase)

$$\delta_i = 180^\circ - \tan^{-1}\left(\frac{h \cos \gamma_i}{R_{CP} - h \sin \gamma_i} \right) \qquad \text{eq. 11}$$

Finally, to calculate the actual steering set-points:

$\alpha_i = \alpha_{Ci} + \delta_i$ (add or subtract 360° as needed for 0-360° range) eq. 12

A working Microsoft Excel model of ***snake mode*** control logic was developed.

Tribot Snake Mode Model

h	17.762	in
γ	0	°

θ	0	120	240
α_{Ci}	0	240	120
γ_i	0	120	240
$h \sin \gamma_i$	0.000	15.382	-15.382
$h \cos \gamma_i$	17.762	-8.881	-8.881

				R_i (in)			δ_i			α_i			V_i		
z	δ_{CL} (°)	R_{CP} (in)	R_{max} (in)	1	2	3	1	2	3	1	2	3	1	2	3
-1.00	90.0	0.000	17.762	17.762	17.762	17.762	90.00	210.00	-30.00	90.00	90.00	90.00	1.00	1.00	1.00
-0.95	85.5	1.398	18.985	17.817	16.566	18.985	85.50	212.42	-27.89	85.50	92.42	92.11	0.94	0.87	1.00
-0.90	81.0	2.813	20.247	17.983	15.390	20.247	81.00	215.24	-26.02	81.00	95.24	93.98	0.89	0.76	1.00
-0.85	76.5	4.264	21.561	18.267	14.230	21.561	76.50	218.62	-24.32	76.50	98.62	95.68	0.85	0.66	1.00
-0.80	72.0	5.771	22.942	18.676	13.086	22.942	72.00	222.74	-22.77	72.00	102.74	97.23	0.81	0.57	1.00
-0.75	67.5	7.357	24.412	19.225	11.970	24.412	67.50	227.90	-21.33	67.50	107.90	98.67	0.79	0.49	1.00
-0.70	63.0	9.050	25.997	19.935	10.907	25.997	63.00	234.51	-19.98	63.00	114.51	100.02	0.77	0.42	1.00
-0.65	58.5	10.885	27.728	20.832	9.955	27.728	58.50	243.14	-18.68	58.50	123.14	101.32	0.75	0.36	1.00
-0.60	54.0	12.905	29.649	21.955	9.220	29.649	54.00	254.41	-17.43	54.00	134.41	102.57	0.74	0.31	1.00
-0.55	49.5	15.170	31.817	23.359	8.884	31.817	49.50	268.63	-16.21	49.50	148.63	103.79	0.73	0.28	1.00
-0.50	45.0	17.762	34.314	25.119	9.194	34.314	45.00	-75.00	-15.00	45.00	165.00	105.00	0.73	0.27	1.00
-0.45	40.5	20.797	37.253	27.349	10.401	37.253	40.50	-58.63	-13.79	40.50	181.37	106.21	0.73	0.28	1.00
-0.40	36.0	24.447	40.808	30.219	12.690	40.808	36.00	-44.41	-12.57	36.00	195.59	107.43	0.74	0.31	1.00
-0.35	31.5	28.985	45.247	33.994	16.245	45.247	31.50	-33.14	-11.32	31.50	206.86	108.68	0.75	0.36	1.00
-0.30	27.0	34.860	51.021	39.124	21.407	51.021	27.00	-24.51	-10.02	27.00	215.49	109.98	0.77	0.42	1.00
-0.25	22.5	42.881	58.937	46.414	28.897	58.937	22.50	-17.90	-8.67	22.50	222.10	111.33	0.79	0.49	1.00
-0.20	18.0	54.666	70.609	57.479	40.275	70.609	18.00	-12.74	-7.23	18.00	227.26	112.77	0.81	0.57	1.00
-0.15	13.5	73.984	89.807	76.086	59.271	89.807	13.50	-8.62	-5.68	13.50	231.38	114.32	0.85	0.66	1.00
-0.10	9.0	112.145	127.836	113.543	97.169	127.836	9.00	-5.24	-3.98	9.00	234.76	116.02	0.89	0.76	1.00
-0.05	4.5	225.688	241.233	226.385	210.493	241.233	4.50	-2.42	-2.11	4.50	237.58	117.89	0.94	0.87	1.00
0.00	0.0	∞	∞	∞	∞	∞	0.00	0.00	0.00	0.00	240.00	120.00	1.00	1.00	1.00
0.05	-4.5	-225.688	241.233	226.385	241.233	210.493	-4.50	2.11	2.42	355.50	242.11	122.42	0.94	1.00	0.87
0.10	-9.0	-112.145	127.836	113.543	127.836	97.169	-9.00	3.98	5.24	351.00	243.98	125.24	0.89	1.00	0.76
0.15	-13.5	-73.984	89.807	76.086	89.807	59.271	-13.50	5.68	8.62	346.50	245.68	128.62	0.85	1.00	0.66
0.20	-18.0	-54.666	70.609	57.479	70.609	40.275	-18.00	7.23	12.74	342.00	247.23	132.74	0.81	1.00	0.57
0.25	-22.5	-42.881	58.937	46.414	58.937	28.897	-22.50	8.67	17.90	337.50	248.67	137.90	0.79	1.00	0.49
0.30	-27.0	-34.860	51.021	39.124	51.021	21.407	-27.00	10.02	24.51	333.00	250.02	144.51	0.77	1.00	0.42
0.35	-31.5	-28.985	45.247	33.994	45.247	16.245	-31.50	11.32	33.14	328.50	251.32	153.14	0.75	1.00	0.36
0.40	-36.0	-24.447	40.808	30.219	40.808	12.690	-36.00	12.57	44.41	324.00	252.57	164.41	0.74	1.00	0.31
0.45	-40.5	-20.797	37.253	27.349	37.253	10.401	-40.50	13.79	58.63	319.50	253.79	178.63	0.73	1.00	0.28
0.50	-45.0	-17.762	34.314	25.119	34.314	9.194	-45.00	15.00	75.00	315.00	255.00	195.00	0.73	1.00	0.27
0.55	-49.5	-15.170	31.817	23.359	31.817	8.884	-49.50	16.21	91.37	310.50	256.21	211.37	0.73	1.00	0.28
0.60	-54.0	-12.905	29.649	21.955	29.649	9.220	-54.00	17.43	105.59	306.00	257.43	225.59	0.74	1.00	0.31
0.65	-58.5	-10.885	27.728	20.832	27.728	9.955	-58.50	18.68	116.86	301.50	258.68	236.86	0.75	1.00	0.36
0.70	-63.0	-9.050	25.997	19.935	25.997	10.907	-63.00	19.98	125.49	297.00	259.98	245.49	0.77	1.00	0.42
0.75	-67.5	-7.357	24.412	19.225	24.412	11.970	-67.50	21.33	132.10	292.50	261.33	252.10	0.79	1.00	0.49
0.80	-72.0	-5.771	22.942	18.676	22.942	13.086	-72.00	22.77	137.26	288.00	262.77	257.26	0.81	1.00	0.57
0.85	-76.5	-4.264	21.561	18.267	21.561	14.230	-76.50	24.32	141.38	283.50	264.32	261.38	0.85	1.00	0.66
0.90	-81.0	-2.813	20.247	17.983	20.247	15.390	-81.00	26.02	144.76	279.00	266.02	264.76	0.89	1.00	0.76
0.95	-85.5	-1.398	18.985	17.817	18.985	16.566	-85.50	27.89	147.58	274.50	267.89	267.58	0.94	1.00	0.87
1.00	-90.0	0.000	17.762	17.762	17.762	17.762	270.00	30.00	150.00	270.00	270.00	270.00	1.00	1.00	1.00

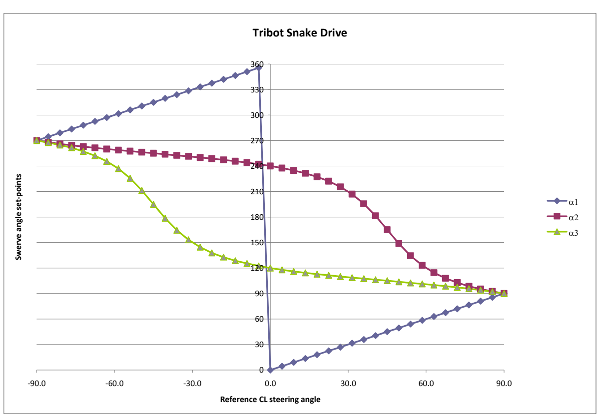

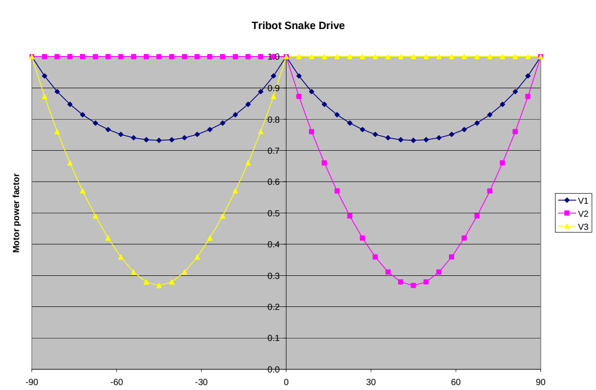

Chassis-centric Ocelot Mode

Presently, ***ocelot mode*** requires that the driver dynamically rotate the vector of motion (using the primary joystick) to maintain a steady course while snake steering. This should work with the control equations presented here, although care needs to be taken to keep the turn center-point away from the chassis center-point. Otherwise the robot will spin in a stationary location. I understand that the current ***ocelot drive*** (4-wheel) basically "rolls" along the h radius circle which passes through the pivot axes.

Field-centric Control

Field-centric control requires that the robot be able to sense the direction of the field axis relative to chassis orientation (ϕ). Typically this requires a gyroscope (ideally at the chassis center-point) although other options exist. This sensing need be only one axis.

If using a gyroscope, concerns are:

1. Stability of the gyroscope over the match duration
2. Initializing and calibrating the control system to the field axis at match start.

We need to understand what chassis orientation behavior we want in field-centric control. We know from chassis-centric experience that the orientation relative to the field changes as we drive. We could accept this; using the gyroscope to control speed and direction relative to the field but allow orientation to drift as we drive and then control it using the secondary joystick only as and when needed, or we could use the gyroscope data to control chassis orientation unless the secondary joystick is used to change it.

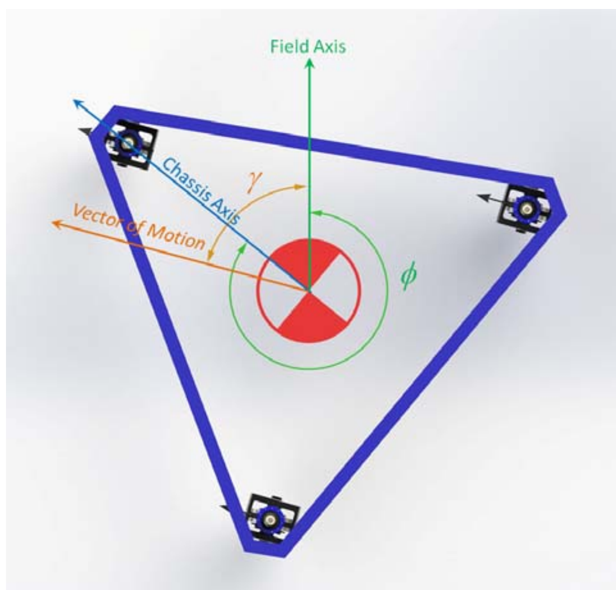

Field-centric Crab Mode

There needs to be an additional piece of information: ϕ (°), the angular displacement of the field axis from the chassis axis (0-360°).

The joystick steering direction, γ (°), is now relative to the field axis, not the chassis axis.

For crab mode, swerve set-points can be calculated:

$$\alpha_{C1} = \gamma + \phi \qquad \text{eq. 13}$$

$$\alpha_{C2} = \gamma + \phi - 120° \qquad \text{eq. 14}$$

$$\alpha_{C3} = \gamma + \phi - 240° \qquad \text{eq. 15}$$

As with chassis-centric crab mode, these values need to be checked and adjusted to 0-360° range.

All drive motors are driven at the same power on ***crab mode*** based on primary joystick displacement from neutral.

Field-Centric Chassis Orientation

The action of the secondary joystick is fundamentally different in field-centric control than it is in chassis-centric. In chassis-centric control, this input drives the robot in ***snake*** turns. In field-centric, the secondary joystick rotates the chassis to change chassis orientation while driving in ***crab mode***. This is an ***ocelot twist*** and this drive mode is automatic in field-centric control. In chassis-centric, ***ocelot twist*** driving requires dynamic driver control. In field-centric control, it is ***snake turning*** which requires dynamic driver control. They are flipped.

The white paper *"Pivot-Wheel Drive - Crab with a Twist"* of 29-March-2010 dealt with ***ocelot mode*** (referred to as Twist 2 in the paper), but not effectively. A different approach is used here.

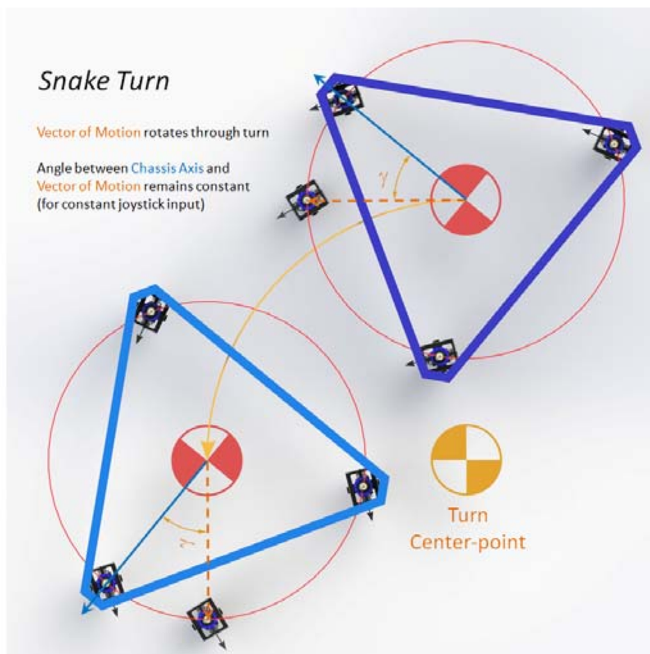

Actually, an ***ocelot*** twist is handled just like a ***snake*** turn, but with a critical difference:

- In a ***snake*** turn, for a given joystick input, the angle between the *vector of motion* and the chassis axis remains fixed and the *vector of motion* rotates about a turn center-point. Swerve set-points during a ***snake*** turn are static - they are determined by the joystick input only and do not change until the joystick input changes.
- An ***ocelot*** twist, for a given joystick input, maintains a constant *vector of motion* relative to the field axis. While the turn logic and mathematics are the same as snake, an actual turn is prevented by continually adjusting wheel directions to keep the robot's course constant. This is a dynamic steering system.

As with ***snake*** turning, a "reference CL wheel" is used for steering. The steering angle (δ_{CL}) range for this wheel should definitely be constrained to ±45°. δ_{CL} is determined directly by the secondary joystick x input (just as in ***snake***) and determines (for a fixed speed input) the rotational speed of the ***ocelot*** twist. Note that ***ocelot*** twisting will slow the robot's overall velocity and this effect increases as δ_{CL} deviates from 0°.

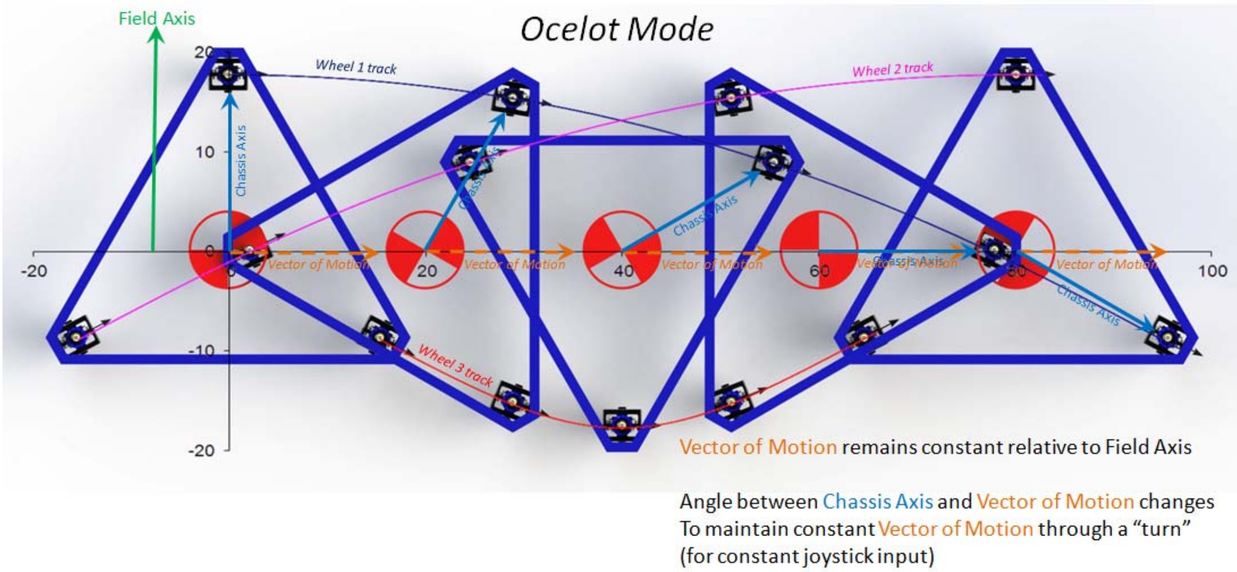

Variables & calculations:

ϕ was defined in the Field-Centric Crab Mode section as the angle between the chassis axis and the field axis. This is provided in real time via on-board instrumentation. It is dynamic.

γ was defined in the Field-Centric Crab Mode section as the steering direction relative to the field axis. This is provided from the primary joystick. Static (as long as joystick input not changed).

α_{C1}, α_{C2} and α_{C3} have been defined in equations 13, 14 & 15 in the Field-Centric Crab Mode section. These are the swerve angle set-points for Field-Centric Crab Mode. Dynamic.

R_{CP} (in) is calculated using equation 4 in the Chassis-Centric Snake Mode section. Even though we're not actually turning, we run the math as if we are. Static (as long as joystick input not changed).

γ_i (defined in the Chassis-Centric Snake Mode section) remains the angular offset between the *vector of motion* and each individual pivot axis (i = 1, 2, 3). Dynamic. The calculation of these values changes under field-centric control:

$\gamma_1 = -\phi - \gamma$ eq. 16

$\gamma_2 = 120° - \phi - \gamma$ eq. 17

$\gamma_3 = 240° - \phi - \gamma$ eq. 18

R_i (in) are the individual wheel distances from the "turn center-point" (i = 1, 2, 3) and are calculated using equation 8. Dynamic.

V_i are the individual wheel power factors (i = 1, 2, 3) and may be calculated using equation 9. Dynamic.

δ_i (°) are the individual swerve angle "corrections" (from the base α_{Ci}'s) needed to affect the ***ocelot*** twist (i = 1, 2, 3). Calculated from equation 10 and are not conditional as long as $-45° \le \delta_{CL} \le +45°$. Dynamic.

α_i (°) are the swerve angle set-points (i = 1, 2, 3). Calculated using equation 12. Dynamic.

So almost all of the mathematics are recycled from ***snake mode***.

A robust Microsoft Excel model of field-centric ***ocelot mode*** control logic was developed, but it's a little heavy to paste in a Microsoft Word document. An observation is warranted, though. The plots of δ_i versus γ_i and V_i versus γ_i are very characteristic and regular for a given δ_{CL}. Examples below. There may be an opportunity to reduce some calculation burden with look-up tables. Something to keep in mind.

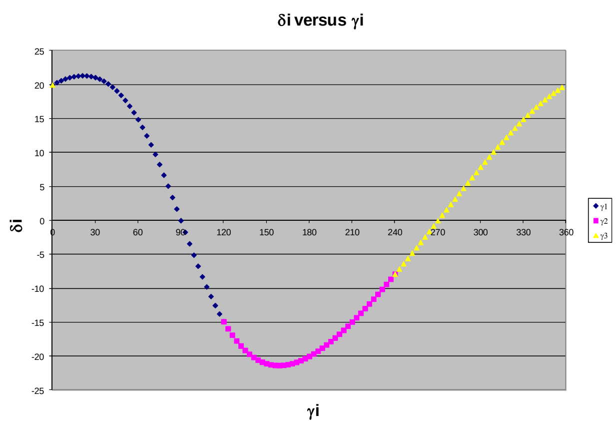

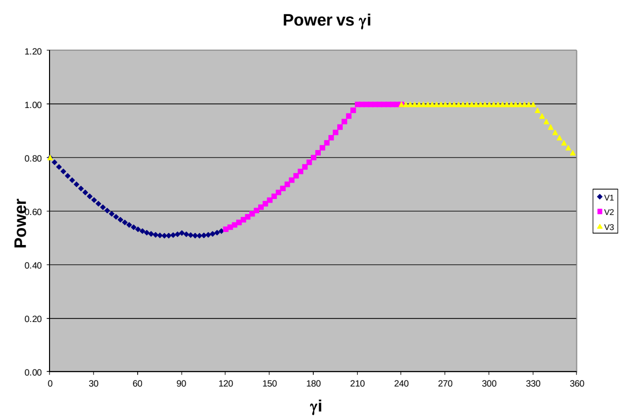

More on the above two charts

The above charts provide an indication that δ_i's could be stored in a look-up table as a function of γ_i and δ_{CL}. This in fact seems to be the case.

The next set of charts (top of the following page) examines the affect of negating δ_{CL} on δ_i and V_i. If there is a simple relationship between negated δ_{CL}'s (a reasonable expectation), then the look-up tables could be cut to half the size (for the same performance).

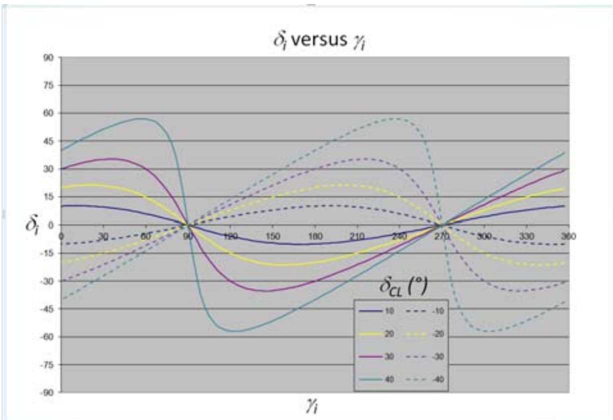

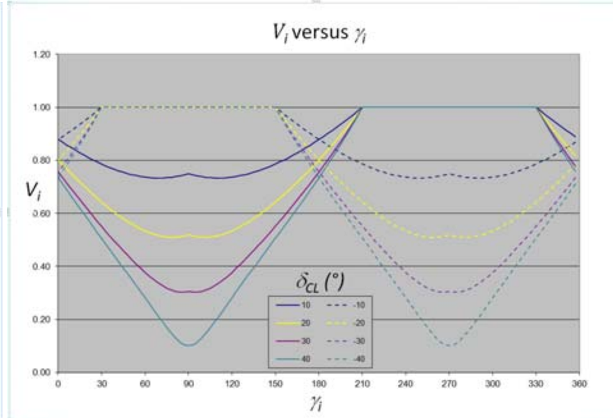

When δ_{CL} is negated, the affect on both δ_i and V_i is a phase shift in γ_i of 180°. So, a look-up table having only positive (or only negative) δ_{CL}*'s* can be used to cover the entire turning range, but for negative δ_{CL}*'s*, the γ_i look-up would need to be shifted by 180° (and checked for 0-360° range).

Looking at positive δ_{CL}*'s* only in the range from 5° to 45° using 5° increments of δ_{CL} and 3° steps of γ_i, δ_i and V_i were calculated (at fixed *h* = 17.762 in) and shown below.

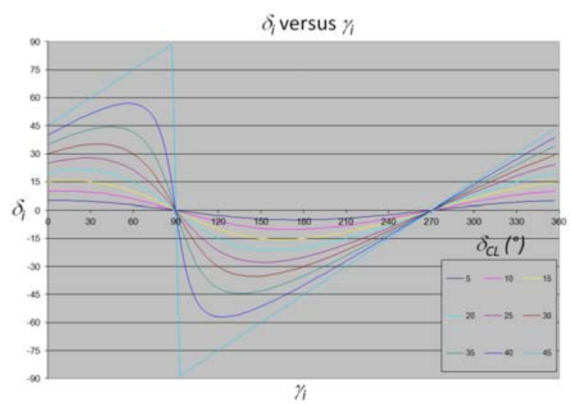

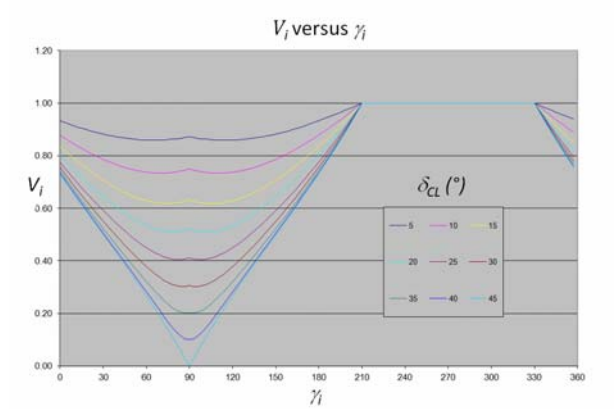

The tables of calculated values of δ_i and V_i are provided at the end of this paper.

A Final Twist in our Story

The final twist is a stationary twist around the chassis center-point. Swerve angles would all be 90° or 270°, depending upon the direction of the twist. We do this now (DEWBOT X). We'll need to do it with a 3-swerve robot as well. This is referred to as Twist 3 in *"Pivot-Wheel Drive - Crab with a Twist"* of 29-March-2010.

δ_{CL} (°):	5	10	15	20	25	30	35	40	45	5	10	15	20	25	30	35	40	45
γ_i					δ_i									V_i				
360	5.00	10.00	15.00	20.00	25.00	30.00	35.00	40.00	45.00	0.932	0.878	0.835	0.801	0.775	0.756	0.743	0.735	0.732
357	4.97	9.90	14.78	19.63	24.45	29.23	34.00	38.75	43.50	0.939	0.889	0.850	0.820	0.796	0.778	0.766	0.759	0.757
354	4.93	9.77	14.53	19.22	23.85	28.44	32.98	37.50	42.00	0.945	0.901	0.866	0.838	0.817	0.801	0.790	0.783	0.781
351	4.87	9.62	14.25	18.78	23.23	27.61	31.94	36.23	40.50	0.951	0.912	0.881	0.857	0.838	0.824	0.814	0.809	0.807
348	4.80	9.45	13.94	18.31	22.58	26.76	30.87	34.95	39.00	0.958	0.924	0.897	0.876	0.859	0.847	0.839	0.834	0.832
345	4.72	9.25	13.61	17.81	21.90	25.88	29.79	33.66	37.50	0.965	0.936	0.913	0.895	0.882	0.871	0.864	0.860	0.859
342	4.63	9.04	13.24	17.28	21.19	24.98	28.70	32.36	36.00	0.972	0.949	0.930	0.916	0.904	0.896	0.890	0.887	0.886
339	4.53	8.80	12.86	16.73	20.46	24.07	27.59	31.06	34.50	0.979	0.961	0.947	0.936	0.927	0.921	0.917	0.914	0.913
336	4.41	8.55	12.45	16.15	19.70	23.13	26.47	29.75	33.00	0.986	0.974	0.964	0.957	0.951	0.947	0.944	0.942	0.941
333	4.29	8.28	12.02	15.55	18.93	22.18	25.33	28.43	31.50	0.993	0.987	0.982	0.978	0.975	0.973	0.971	0.971	0.970
330	4.15	7.99	11.57	14.93	18.13	21.21	24.19	27.11	30.00	1.000	1.000	1.000	1.000	1.000	1.000	1.000	1.000	1.000
327	4.01	7.68	11.10	14.29	17.32	20.22	23.03	25.78	28.50	1.000	1.000	1.000	1.000	1.000	1.000	1.000	1.000	1.000
324	3.85	7.36	10.61	13.63	16.49	19.23	21.87	24.45	27.00	1.000	1.000	1.000	1.000	1.000	1.000	1.000	1.000	1.000
321	3.69	7.03	10.10	12.96	15.65	18.22	20.69	23.11	25.50	1.000	1.000	1.000	1.000	1.000	1.000	1.000	1.000	1.000
318	3.51	6.69	9.58	12.27	14.80	17.20	19.51	21.77	24.00	1.000	1.000	1.000	1.000	1.000	1.000	1.000	1.000	1.000
315	3.33	6.33	9.05	11.57	13.93	16.17	18.32	20.42	22.50	1.000	1.000	1.000	1.000	1.000	1.000	1.000	1.000	1.000
312	3.15	5.96	8.50	10.85	13.05	15.13	17.13	19.08	21.00	1.000	1.000	1.000	1.000	1.000	1.000	1.000	1.000	1.000
309	2.95	5.57	7.95	10.12	12.16	14.08	15.93	17.73	19.50	1.000	1.000	1.000	1.000	1.000	1.000	1.000	1.000	1.000
306	2.75	5.18	7.38	9.38	11.26	13.02	14.72	16.37	18.00	1.000	1.000	1.000	1.000	1.000	1.000	1.000	1.000	1.000
303	2.54	4.78	6.80	8.64	10.35	11.96	13.51	15.02	16.50	1.000	1.000	1.000	1.000	1.000	1.000	1.000	1.000	1.000
300	2.33	4.37	6.21	7.88	9.43	10.89	12.29	13.66	15.00	1.000	1.000	1.000	1.000	1.000	1.000	1.000	1.000	1.000
297	2.11	3.96	5.61	7.11	8.51	9.82	11.08	12.30	13.50	1.000	1.000	1.000	1.000	1.000	1.000	1.000	1.000	1.000
294	1.89	3.53	5.00	6.34	7.58	8.74	9.85	10.93	12.00	1.000	1.000	1.000	1.000	1.000	1.000	1.000	1.000	1.000
291	1.66	3.11	4.39	5.56	6.64	7.66	8.63	9.57	10.50	1.000	1.000	1.000	1.000	1.000	1.000	1.000	1.000	1.000
288	1.43	2.67	3.78	4.78	5.70	6.57	7.40	8.21	9.00	1.000	1.000	1.000	1.000	1.000	1.000	1.000	1.000	1.000
285	1.20	2.23	3.15	3.99	4.76	5.48	6.17	6.84	7.50	1.000	1.000	1.000	1.000	1.000	1.000	1.000	1.000	1.000
282	0.96	1.79	2.53	3.19	3.81	4.39	4.94	5.47	6.00	1.000	1.000	1.000	1.000	1.000	1.000	1.000	1.000	1.000
279	0.72	1.35	1.90	2.40	2.86	3.29	3.70	4.11	4.50	1.000	1.000	1.000	1.000	1.000	1.000	1.000	1.000	1.000
276	0.48	0.90	1.27	1.60	1.91	2.20	2.47	2.74	3.00	1.000	1.000	1.000	1.000	1.000	1.000	1.000	1.000	1.000
273	0.24	0.45	0.63	0.80	0.95	1.10	1.24	1.37	1.50	1.000	1.000	1.000	1.000	1.000	1.000	1.000	1.000	1.000
270	0.00	0.00	0.00	0.00	0.00	0.00	0.00	0.00	0.00	1.000	1.000	1.000	1.000	1.000	1.000	1.000	1.000	1.000
267	-0.24	-0.45	-0.63	-0.80	-0.95	-1.10	-1.24	-1.37	-1.50	1.000	1.000	1.000	1.000	1.000	1.000	1.000	1.000	1.000
264	-0.48	-0.90	-1.27	-1.60	-1.91	-2.20	-2.47	-2.74	-3.00	1.000	1.000	1.000	1.000	1.000	1.000	1.000	1.000	1.000
261	-0.72	-1.35	-1.90	-2.40	-2.86	-3.29	-3.70	-4.11	-4.50	1.000	1.000	1.000	1.000	1.000	1.000	1.000	1.000	1.000
258	-0.96	-1.79	-2.53	-3.19	-3.81	-4.39	-4.94	-5.47	-6.00	1.000	1.000	1.000	1.000	1.000	1.000	1.000	1.000	1.000
255	-1.20	-2.23	-3.15	-3.99	-4.76	-5.48	-6.17	-6.84	-7.50	1.000	1.000	1.000	1.000	1.000	1.000	1.000	1.000	1.000
252	-1.43	-2.67	-3.78	-4.78	-5.70	-6.57	-7.40	-8.21	-9.00	1.000	1.000	1.000	1.000	1.000	1.000	1.000	1.000	1.000
249	-1.66	-3.11	-4.39	-5.56	-6.64	-7.66	-8.63	-9.57	-10.50	1.000	1.000	1.000	1.000	1.000	1.000	1.000	1.000	1.000
246	-1.89	-3.53	-5.00	-6.34	-7.58	-8.74	-9.85	-10.93	-12.00	1.000	1.000	1.000	1.000	1.000	1.000	1.000	1.000	1.000
243	-2.11	-3.96	-5.61	-7.11	-8.51	-9.82	-11.08	-12.30	-13.50	1.000	1.000	1.000	1.000	1.000	1.000	1.000	1.000	1.000

δ_{CL} (°):	5	10	15	20	25	30	35	40	45	5	10	15	20	25	30	35	40	45
γ_i					δ_i									V_i				
240	-2.33	-4.37	-6.21	-7.88	-9.43	-10.89	-12.29	-13.66	-15.00	1.000	1.000	1.000	1.000	1.000	1.000	1.000	1.000	1.000
237	-2.54	-4.78	-6.80	-8.64	-10.35	-11.96	-13.51	-15.02	-16.50	1.000	1.000	1.000	1.000	1.000	1.000	1.000	1.000	1.000
234	-2.75	-5.18	-7.38	-9.38	-11.26	-13.02	-14.72	-16.37	-18.00	1.000	1.000	1.000	1.000	1.000	1.000	1.000	1.000	1.000
231	-2.95	-5.57	-7.95	-10.12	-12.16	-14.08	-15.93	-17.73	-19.50	1.000	1.000	1.000	1.000	1.000	1.000	1.000	1.000	1.000
228	-3.15	-5.96	-8.50	-10.85	-13.05	-15.13	-17.13	-19.08	-21.00	1.000	1.000	1.000	1.000	1.000	1.000	1.000	1.000	1.000
225	-3.33	-6.33	-9.05	-11.57	-13.93	-16.17	-18.32	-20.42	-22.50	1.000	1.000	1.000	1.000	1.000	1.000	1.000	1.000	1.000
222	-3.51	-6.69	-9.58	-12.27	-14.80	-17.20	-19.51	-21.77	-24.00	1.000	1.000	1.000	1.000	1.000	1.000	1.000	1.000	1.000
219	-3.69	-7.03	-10.10	-12.96	-15.65	-18.22	-20.69	-23.11	-25.50	1.000	1.000	1.000	1.000	1.000	1.000	1.000	1.000	1.000
216	-3.85	-7.36	-10.61	-13.63	-16.49	-19.23	-21.87	-24.45	-27.00	1.000	1.000	1.000	1.000	1.000	1.000	1.000	1.000	1.000
213	-4.01	-7.68	-11.10	-14.29	-17.32	-20.22	-23.03	-25.78	-28.50	1.000	1.000	1.000	1.000	1.000	1.000	1.000	1.000	1.000
210	-4.15	-7.99	-11.57	-14.93	-18.13	-21.21	-24.19	-27.11	-30.00	1.000	1.000	1.000	1.000	1.000	1.000	1.000	1.000	1.000
207	-4.29	-8.28	-12.02	-15.55	-18.93	-22.18	-25.33	-28.43	-31.50	0.993	0.987	0.982	0.978	0.975	0.973	0.971	0.971	0.970
204	-4.41	-8.55	-12.45	-16.15	-19.70	-23.13	-26.47	-29.75	-33.00	0.986	0.974	0.964	0.957	0.951	0.947	0.944	0.942	0.941
201	-4.53	-8.80	-12.86	-16.73	-20.46	-24.07	-27.59	-31.06	-34.50	0.979	0.961	0.947	0.936	0.927	0.921	0.917	0.914	0.913
198	-4.63	-9.04	-13.24	-17.28	-21.19	-24.98	-28.70	-32.36	-36.00	0.972	0.949	0.930	0.916	0.904	0.896	0.890	0.887	0.886
195	-4.72	-9.25	-13.61	-17.81	-21.90	-25.88	-29.79	-33.66	-37.50	0.965	0.936	0.913	0.895	0.882	0.871	0.864	0.860	0.859
192	-4.80	-9.45	-13.94	-18.31	-22.58	-26.76	-30.87	-34.95	-39.00	0.958	0.924	0.897	0.876	0.859	0.847	0.839	0.834	0.832
189	-4.87	-9.62	-14.25	-18.78	-23.23	-27.61	-31.94	-36.23	-40.50	0.951	0.912	0.881	0.857	0.838	0.824	0.814	0.809	0.807
186	-4.93	-9.77	-14.53	-19.22	-23.85	-28.44	-32.98	-37.50	-42.00	0.945	0.901	0.866	0.838	0.817	0.801	0.790	0.783	0.781
183	-4.97	-9.90	-14.78	-19.63	-24.45	-29.23	-34.00	-38.75	-43.50	0.939	0.889	0.850	0.820	0.796	0.778	0.766	0.759	0.757
180	-5.00	-10.00	-15.00	-20.00	-25.00	-30.00	-35.00	-40.00	-45.00	0.932	0.878	0.835	0.801	0.775	0.756	0.743	0.735	0.732
177	-5.02	-10.08	-15.18	-20.33	-25.52	-30.73	-35.97	-41.23	-46.50	0.926	0.868	0.821	0.784	0.755	0.734	0.719	0.711	0.708
174	-5.02	-10.13	-15.33	-20.62	-25.99	-31.43	-36.92	-42.45	-48.00	0.921	0.857	0.807	0.767	0.736	0.713	0.697	0.687	0.684
171	-5.01	-10.15	-15.44	-20.87	-26.42	-32.08	-37.84	-43.65	-49.50	0.915	0.847	0.793	0.750	0.716	0.691	0.674	0.664	0.661
168	-4.98	-10.15	-15.51	-21.06	-26.80	-32.69	-38.72	-44.83	-51.00	0.910	0.837	0.779	0.733	0.697	0.671	0.652	0.641	0.637
165	-4.94	-10.12	-15.54	-21.21	-27.12	-33.25	-39.56	-46.00	-52.50	0.904	0.828	0.766	0.717	0.679	0.650	0.630	0.618	0.614
162	-4.89	-10.06	-15.53	-21.31	-27.39	-33.76	-40.36	-47.13	-54.00	0.899	0.819	0.754	0.701	0.661	0.630	0.608	0.595	0.591
159	-4.82	-9.97	-15.47	-21.34	-27.60	-34.20	-41.11	-48.25	-55.50	0.895	0.810	0.741	0.686	0.643	0.610	0.587	0.573	0.568
156	-4.74	-9.84	-15.36	-21.32	-27.73	-34.58	-41.81	-49.33	-57.00	0.890	0.801	0.729	0.671	0.625	0.590	0.565	0.550	0.545
153	-4.64	-9.69	-15.21	-21.23	-27.79	-34.88	-42.45	-50.37	-58.50	0.886	0.794	0.718	0.657	0.608	0.570	0.544	0.528	0.523
150	-4.53	-9.51	-15.00	-21.07	-27.77	-35.10	-43.02	-51.38	-60.00	0.882	0.786	0.707	0.643	0.591	0.551	0.523	0.506	0.500
147	-4.41	-9.29	-14.74	-20.84	-27.66	-35.23	-43.51	-52.35	-61.50	0.878	0.779	0.697	0.629	0.575	0.532	0.502	0.483	0.477
144	-4.27	-9.04	-14.43	-20.54	-27.46	-35.26	-43.91	-53.26	-63.00	0.875	0.772	0.687	0.616	0.559	0.514	0.481	0.461	0.455
141	-4.12	-8.76	-14.06	-20.15	-27.15	-35.17	-44.21	-54.11	-64.50	0.872	0.766	0.677	0.604	0.543	0.495	0.460	0.439	0.432
138	-3.95	-8.45	-13.64	-19.68	-26.73	-34.96	-44.39	-54.88	-66.00	0.869	0.760	0.668	0.592	0.528	0.477	0.440	0.417	0.409
135	-3.77	-8.11	-13.16	-19.11	-26.19	-34.60	-44.44	-55.57	-67.50	0.867	0.755	0.660	0.580	0.513	0.459	0.419	0.394	0.386
132	-3.58	-7.73	-12.62	-18.46	-25.52	-34.08	-44.33	-56.16	-69.00	0.865	0.750	0.653	0.569	0.499	0.442	0.399	0.372	0.363
129	-3.38	-7.33	-12.02	-17.71	-24.71	-33.39	-44.03	-56.62	-70.50	0.863	0.746	0.646	0.559	0.486	0.425	0.379	0.350	0.339
126	-3.17	-6.89	-11.37	-16.87	-23.76	-32.49	-43.51	-56.93	-72.00	0.861	0.742	0.639	0.550	0.473	0.409	0.359	0.327	0.316
123	-2.94	-6.43	-10.66	-15.93	-22.64	-31.37	-42.74	-57.05	-73.50	0.860	0.739	0.634	0.541	0.461	0.393	0.340	0.304	0.292

δ_{CL} (°):	5	10	15	20	25	30	35	40	45	5	10	15	20	25	30	35	40	45
γ_i					δ_i									V_i				
120	-2.71	-5.94	-9.90	-14.88	-21.36	-30.00	-41.65	-56.92	-75.00	0.859	0.737	0.629	0.534	0.450	0.378	0.320	0.282	0.268
117	-2.47	-5.43	-9.08	-13.74	-19.91	-28.36	-40.20	-56.48	-76.50	0.859	0.735	0.625	0.527	0.440	0.364	0.302	0.259	0.243
114	-2.21	-4.89	-8.21	-12.50	-18.28	-26.42	-38.32	-55.63	-78.00	0.859	0.734	0.622	0.521	0.430	0.350	0.284	0.236	0.219
111	-1.96	-4.33	-7.30	-11.18	-16.49	-24.17	-35.93	-54.23	-79.50	0.859	0.733	0.620	0.516	0.423	0.338	0.266	0.214	0.193
108	-1.69	-3.75	-6.34	-9.76	-14.52	-21.59	-32.93	-52.08	-81.00	0.860	0.733	0.618	0.513	0.416	0.328	0.250	0.191	0.168
105	-1.42	-3.15	-5.35	-8.27	-12.39	-18.67	-29.25	-48.89	-82.50	0.861	0.734	0.618	0.511	0.411	0.318	0.236	0.170	0.141
102	-1.14	-2.54	-4.32	-6.70	-10.11	-15.42	-24.80	-44.23	-84.00	0.862	0.736	0.619	0.510	0.407	0.311	0.223	0.149	0.114
99	-0.86	-1.91	-3.26	-5.08	-7.70	-11.87	-19.55	-37.47	-85.50	0.864	0.738	0.620	0.510	0.405	0.306	0.213	0.130	0.087
96	-0.57	-1.28	-2.19	-3.41	-5.19	-8.07	-13.55	-27.92	-87.00	0.866	0.741	0.623	0.512	0.405	0.303	0.205	0.114	0.059
93	-0.29	-0.64	-1.10	-1.71	-2.62	-4.08	-6.95	-15.16	-88.50	0.869	0.745	0.627	0.515	0.407	0.303	0.202	0.104	0.030
90	0.00	0.00	0.00	0.00	0.00	0.00	0.00	0.00	17.03	0.872	0.750	0.632	0.520	0.411	0.306	0.203	0.101	0.000
87	0.29	0.64	1.10	1.71	2.62	4.08	6.95	15.16	88.50	0.869	0.745	0.627	0.515	0.407	0.303	0.202	0.104	0.030
84	0.57	1.28	2.19	3.41	5.19	8.07	13.55	27.92	87.00	0.866	0.741	0.623	0.512	0.405	0.303	0.205	0.114	0.059
81	0.86	1.91	3.26	5.08	7.70	11.87	19.55	37.47	85.50	0.864	0.738	0.620	0.510	0.405	0.306	0.213	0.130	0.087
78	1.14	2.54	4.32	6.70	10.11	15.42	24.80	44.23	84.00	0.862	0.736	0.619	0.510	0.407	0.311	0.223	0.149	0.114
75	1.42	3.15	5.35	8.27	12.39	18.67	29.25	48.89	82.50	0.861	0.734	0.618	0.511	0.411	0.318	0.236	0.170	0.141
72	1.69	3.75	6.34	9.76	14.52	21.59	32.93	52.08	81.00	0.860	0.733	0.618	0.513	0.416	0.328	0.250	0.191	0.168
69	1.96	4.33	7.30	11.18	16.49	24.17	35.93	54.23	79.50	0.859	0.733	0.620	0.516	0.423	0.338	0.266	0.214	0.193
66	2.21	4.89	8.21	12.50	18.28	26.42	38.32	55.63	78.00	0.859	0.734	0.622	0.521	0.430	0.350	0.284	0.236	0.219
63	2.47	5.43	9.08	13.74	19.91	28.36	40.20	56.48	76.50	0.859	0.735	0.625	0.527	0.440	0.364	0.302	0.259	0.243
60	2.71	5.94	9.90	14.88	21.36	30.00	41.65	56.92	75.00	0.859	0.737	0.629	0.534	0.450	0.378	0.320	0.282	0.268
57	2.94	6.43	10.66	15.93	22.64	31.37	42.74	57.05	73.50	0.860	0.739	0.634	0.541	0.461	0.393	0.340	0.304	0.292
54	3.17	6.89	11.37	16.87	23.76	32.49	43.51	56.93	72.00	0.861	0.742	0.639	0.550	0.473	0.409	0.359	0.327	0.316
51	3.38	7.33	12.02	17.71	24.71	33.39	44.03	56.62	70.50	0.863	0.746	0.646	0.559	0.486	0.425	0.379	0.350	0.339
48	3.58	7.73	12.62	18.46	25.52	34.08	44.33	56.16	69.00	0.865	0.750	0.653	0.569	0.499	0.442	0.399	0.372	0.363
45	3.77	8.11	13.16	19.11	26.19	34.60	44.44	55.57	67.50	0.867	0.755	0.660	0.580	0.513	0.459	0.419	0.394	0.386
42	3.95	8.45	13.64	19.68	26.73	34.96	44.39	54.88	66.00	0.869	0.760	0.668	0.592	0.528	0.477	0.440	0.417	0.409
39	4.12	8.76	14.06	20.15	27.15	35.17	44.21	54.11	64.50	0.872	0.766	0.677	0.604	0.543	0.495	0.460	0.439	0.432
36	4.27	9.04	14.43	20.54	27.46	35.26	43.91	53.26	63.00	0.875	0.772	0.687	0.616	0.559	0.514	0.481	0.461	0.455
33	4.41	9.29	14.74	20.84	27.66	35.23	43.51	52.35	61.50	0.878	0.779	0.697	0.629	0.575	0.532	0.502	0.483	0.477
30	4.53	9.51	15.00	21.07	27.77	35.10	43.02	51.38	60.00	0.882	0.786	0.707	0.643	0.591	0.551	0.523	0.506	0.500
27	4.64	9.69	15.21	21.23	27.79	34.88	42.45	50.37	58.50	0.886	0.794	0.718	0.657	0.608	0.570	0.544	0.528	0.523
24	4.74	9.84	15.36	21.32	27.73	34.58	41.81	49.33	57.00	0.890	0.801	0.729	0.671	0.625	0.590	0.565	0.550	0.545
21	4.82	9.97	15.47	21.34	27.60	34.20	41.11	48.25	55.50	0.895	0.810	0.741	0.686	0.643	0.610	0.587	0.573	0.568
18	4.89	10.06	15.53	21.31	27.39	33.76	40.36	47.13	54.00	0.899	0.819	0.754	0.701	0.661	0.630	0.608	0.595	0.591
15	4.94	10.12	15.54	21.21	27.12	33.25	39.56	46.00	52.50	0.904	0.828	0.766	0.717	0.679	0.650	0.630	0.618	0.614
12	4.98	10.15	15.51	21.06	26.80	32.69	38.72	44.83	51.00	0.910	0.837	0.779	0.733	0.697	0.671	0.652	0.641	0.637
9	5.01	10.15	15.44	20.87	26.42	32.08	37.84	43.65	49.50	0.915	0.847	0.793	0.750	0.716	0.691	0.674	0.664	0.661
6	5.02	10.13	15.33	20.62	25.99	31.43	36.92	42.45	48.00	0.921	0.857	0.807	0.767	0.736	0.713	0.697	0.687	0.684
3	5.02	10.08	15.18	20.33	25.52	30.73	35.97	41.23	46.50	0.926	0.868	0.821	0.784	0.755	0.734	0.719	0.711	0.708
0	5.00	10.00	15.00	20.00	25.00	30.00	35.00	40.00	45.00	0.932	0.878	0.835	0.801	0.775	0.756	0.743	0.735	0.732